

Electrochemical Deposition of Ni-Co/SiC Nanocomposite Coatings for Marine Environment

Baosong Li^{1,*}, Weiwei Zhang²

¹ College of Mechanics and Materials, Hohai University, Nanjing 211100, China

² College of Mechanical and Electrical Engineering, Hohai University, Changzhou 213022, China

*E-mail: bsli@hhu.edu.cn

Received: 28 April 2017 / Accepted: 25 May 2017 / Published: 12 July 2017

Ni-Co/SiC nanocomposite coatings were prepared by electrodeposition from a modified watt type Ni-Co bath containing suspended SiC nanoparticles. The effects of SiC nanoparticles on the structure and morphology of Ni-Co coatings were studied by scanning electron microscopy (SEM), energy spectrum analysis (EDS), X-ray diffraction (XRD) and electrochemical technique. The electrochemical corrosion properties of Ni-Co/SiC composite coatings were studied by EIS and Tafel methods. The results show that the addition of Co²⁺ ions in the bath improves the refinement phase, reduces the porosity and strengthens the corrosion resistance of the nanocomposite deposits. SiC and Co content in the deposits varied with the change of deposition parameters and SiC nanoparticles concentration in the bath. The SiC nanoparticles have the dual role of promoting the nucleation and enhancing the hardness of the Ni-Co alloys which improved the wear resistance of the Ni-Co/SiC coatings. The incorporation of SiC nanoparticles into Ni-Co alloy matrix alters the chemical composition, increases the microhardness, significantly enhances the anti-corrosion behavior and wear resistance of the composite coatings. The composite coatings can provide long-term protection for metal parts in marine environment and have a good application prospect in the field of marine protection.

Keywords: Ni-Co/SiC nanocomposite coatings; Electrodeposition; wear resistance; corrosion behavior; marine protection

1. INTRODUCTION

The deterioration of service performance of metal parts in marine environment will be accelerated by the interaction of corrosion, erosion, microbial contamination and other factors. In recent years, nanocomposite coatings with enhanced physical, mechanical, corrosion and tribological properties, have been prepared through co-deposition of functional nanoparticles in metal matrix

coatings. During the co-deposition process, the reinforcing particles, which suspended in the electrolyte, are embedded in the growing metal or alloy matrix [1-3]. Ni-Co alloys are well-known owing to their favorable properties such as good corrosion resistance, wear resistance, mechanical performance, thermal stability and magnetism [4-6]. These special characteristics have made them widely employed as alloy matrix in metal surface protection [7-9]. Various nanoparticles have been incorporated into alloy matrix through electrochemical methods, such as Al_2O_3 , TiO_2 , SiO_2 , diamond, WC, SiC, Cr_2O_3 and Si_3N_4 [10-11], to obtain special performance. SiC nanoparticles are frequently used as second-phase reinforcing particles in composite coatings to improve the wear resistance due to their excellent thermal stability, high hardness, commercially available and oxidation resistant [12-17]. Since the nanocomposite coatings have the advantages of both the electrodeposited alloys and the hard nanoparticles [10, 18], it can be expected that SiC nanoparticles could substantially enhance the properties of Ni-Co coatings, including its mechanical, tribological and anti-corrosion behavior [19-22].

Till now, many valuable literatures have reported on the electrochemical co-deposition of nanocomposite coatings and their physicochemical properties. However, the co-deposition mechanism of inert particles is not yet fully understood. The major challenge is how to prevent nanoparticles from agglomeration. Owing to the agglomeration, insolubility and nonconductive of the suspended particles in the bath, the co-deposition mechanism of the dispersion of inert particles into metallic matrix has been rarely reported conformably and is still not entirely understood. The microstructure, physical and mechanical properties of nanocomposite coatings is affected by SiC content, electrodeposition parameters including deposition time and current density. Therefore, it is essential to investigate the effects of deposition parameters, such as embedded nanoparticles content, current density, deposition time on the microstructure of the resulting nanocomposites.

Thus, in the present work, the co-deposition of SiC nanoparticles with Ni-Co matrix by a simple and valuable, low-temperature electrochemical co-deposition technique was studied. The impacts of co-deposition parameters and SiC nanoparticles on the composition, microstructure, morphology and electrochemical properties of the Ni-Co/SiC nanocomposite coatings were evaluated. The relationship between SiC incorporation and final performance such as the corrosion and wear resistance of the deposited Ni-Co/SiC nanocomposite was discussed. The corrosion resistance of the coatings in 3.5% NaCl solution was investigated.

2. EXPERIMENTAL

The electrolyte compositions and electrodeposition parameters are shown in Table 1. Analytical reagents and distilled water were employed to prepare the electrolyte. SiC were used without any pre-treatment. In order to prevent the agglomeration of the SiC particles and maintain it in suspension state, the electrolytes containing the SiC particles were premixed and stirred by continuous magnetic stirrer for at least 24 h. During the electrodeposition process, the electrolyte was also stirred mechanically to maintain a uniform concentration of particles in the bulk solution. A nickel plates was used as anode. The cathodes were copper plates. The electrodes were positioned vertically in a 250 ml

electrodeposition baths. The distance between anode and cathode was 35 mm. In order to provide suitable substrate surface for electrodeposition, cathodes were mechanically polished to 1200-grit finish with SiC abrasive papers. Thereafter, they were cleaned ultrasonically in the acetone and ethanol consecutively about 10 min, washed in distilled water and then immersed immediately in the plating bath. The pH of the electrolyte was 4.2 and the temperature was kept constant at 35°C. The coatings were cleaned ultrasonically for 5 min after the electrodeposition to remove the loosely adsorbed SiC nanoparticles from the surface.

A scanning electron microscope (SEM, model HITACHI-S3400N) was used to investigate the surface morphologies of the composite coatings. The weight percentage of SiC in the coatings was determined with Oxford INCA energy dispersive X-ray spectroscopy (EDS) coupled to the SEM. XRD analysis was carried out with a D8 Advance model X-ray diffractometer operated at 40 kV and 300 mA with Cu-K α radiation ($\lambda=1.5406 \text{ \AA}$) to determine the phase structure and preferred orientation of the deposits. All electrochemical experiments were performed in a typical three-electrode cell using a CHI 660E electrochemical working station in 3.5% NaCl corrosive medium without agitation at the room temperature (25 °C). The reference electrode was a saturated calomel electrode (SCE), and the counter electrode was a platinum electrode. The bath was deoxidized 20 min by Nitrogen before experiment. Immersion test was performed in the neutral 3.5 wt.% NaCl solutions for 1 to 30 days at open circuit potential at room temperature. Then, EIS was performed at open circuit potential with amplitude 10mV in an applied frequency ranged from 10^5 Hz down to 10^{-2} Hz when the coatings have been immersed for 1, 3, 7, 10, 15, 20, 30 days. And the potentiodynamic polarization tests of the immersed coatings were also measured at a sweep rate of 1 mV/s in 3.5% NaCl solution at room temperature.

Table 1. Bath composition and co-deposition parameters of Ni-Co/SiC nanocomposite coatings.

bath composition (g/L)		co-deposition parameters	
NiSO ₄ ·6H ₂ O	200	pH	4.2
NiCl ₂	20	Temperature	35 °C
CoSO ₄ ·7H ₂ O	20	Current density	0.5-4 ·dm ⁻²
H ₃ BO ₃	30	Agitation rate	360 rpm
NaCl	10	Electrode distance	35 mm
SiC nanoparticles	0-5	Anode	Ni plates
SiC average size	80-150 nm		

3. RESULTS AND DISCUSSION

3.1 Electrodeposition and morphologies of the Ni-W, Ni-W/SiC composite coatings

In order to investigate the effects of SiC nanoparticles on the properties of Ni-Co/SiC composite coatings, as contrast samples, the Ni-Co alloys were deposited at the same deposition parameters with Ni-Co/SiC except for SiC concentration. Fig.1 shows that the surface morphology of Ni-Co alloys obtained with different concentration of CoSO₄ at current density 1.32 A / dm² for 3 min.

It can be seen from Fig.1, the coating becomes finer and even with the increase of CoSO_4 content in the bath. When CoSO_4 concentration is 20 g/L, the size of crystal grain is 0.6-1.5 μm , and the surface is partly concave and uneven. When the concentration of CoSO_4 is 40 g/L, the crystal is obviously reduced to about 0.3-0.5 μm . Continue to increase the concentration of CoSO_4 to 80 g/L, the crystal size decreases to 0.1-0.2 μm . Bakhit [23] reported that the cobalt content and SiC nanoparticle content were increased by increasing the cobalt concentration. Adding cobalt into the bath enhanced particle incorporation considerably. As shown in Fig.1, the dispersion of Co content in the deposits was uniform. It indicated that Co^{2+} ions have obvious effect on the structure and morphology of the nanocomposite coating. Co^{2+} ions can refine the crystal, improve the evenness and enhance the corrosion resistance of the coating.

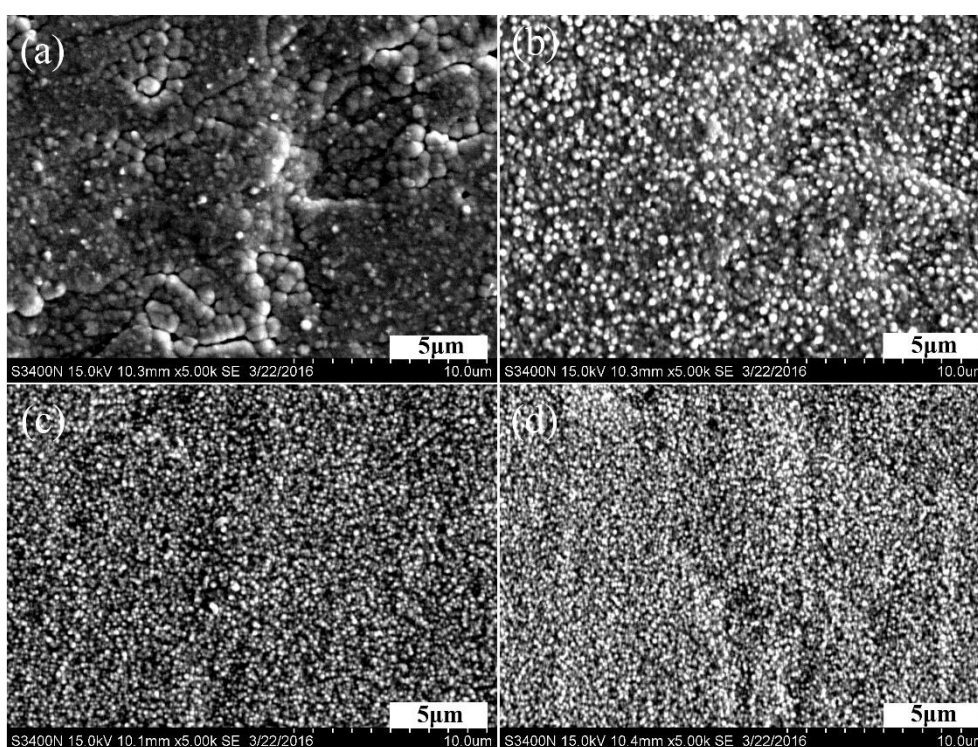


Figure 1. SEM images of the Ni-Co alloys with different CoSO_4 concentration in the bath (a) 20, (b) 40, (c) 60 and (d) 80 g/L, $i = 1.32 \text{ A / dm}^2$, $t = 3 \text{ min}$.

Garcia, et al [24] found that the size and number density of SiC particles in the plating solution are important parameters in the codeposition process, and the decrease in the particle size affects the wear resistance in a positive way. Therefore, the nanoparticles of SiC were employed for reinforcing the coatings in this work. Fig. 2 is the morphologies of the Ni-Co/SiC nanocomposite coatings after addition of 1.5 g/L SiC into the bath. The diameter of SiC nanoparticle is 120 nm. To prevent the agglomeration of the SiC nanoparticles, the electrolytes were premixed and mechanically stirred for 24 hours. As Fig. 2 shown, a large number of SiC nanoparticles are embedded in the coatings which is smooth, crack free and compact. The presence of SiC nanoparticles in electrolyte affects the Ni-Co alloy deposition in many ways [25, 26]. Dispersing and embedding of SiC nanoparticles into the

growing metal matrix results in the decrease of active cathode surface. In the co-deposition process, many SiC nanoparticles are incorporated in Ni-Co deposited matrix. The amount of co-deposited SiC increases with the increase of SiC concentration in the bath till up to a certain SiC concentration. These results is consistent with the report previously [27,28]. The surface of the composite coatings was smooth and shiny, with a few agglomerations on it. More SiC concentration will lead to agglomeration. Less agglomeration and more uniform distribution of nanoparticles within the metal matrix were formed for the deposit from the bath containing 1.5 g/L SiC.

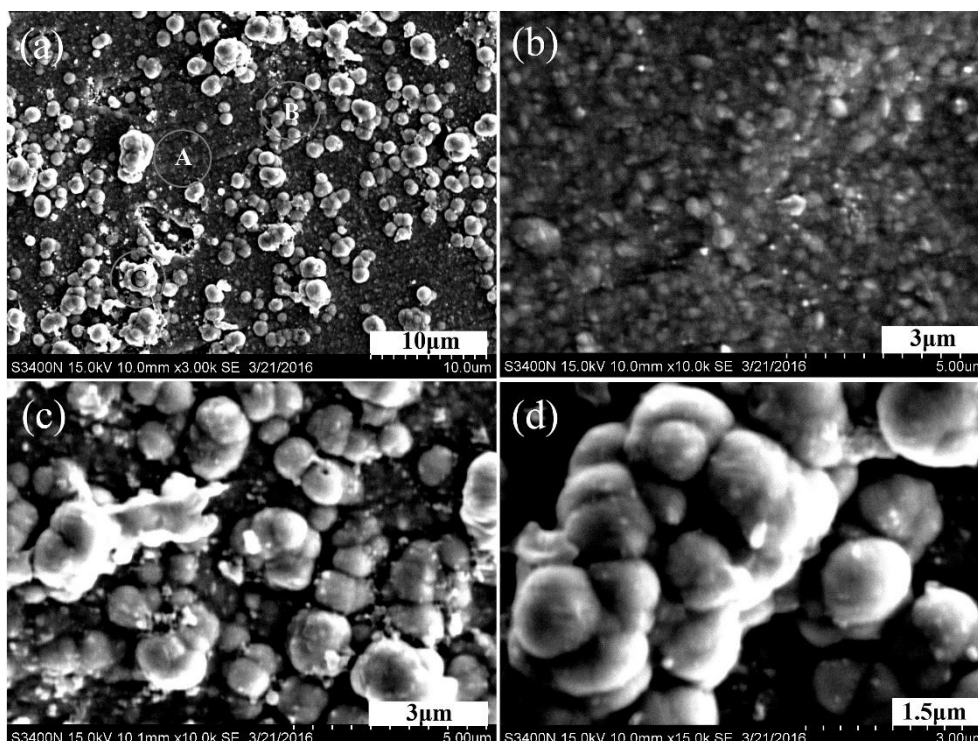


Figure 2. SEM images of the Ni-Co/SiC alloys (a), and enlarged images corresponding to the designated region (b) A, (c) B, and (d) C, SiC 1.5 g/L, $i = 1.32 \text{ A / dm}^2$, $t = 3 \text{ min}$.

As seen in Fig. 2(a), the surface is composed of three regions according to the microstructure and morphologies of the nanocomposite coatings. The designated region A has less agglomerations, the surface is flat and compact, no crack, low porosity. The EDS analysis shows that the imbedded SiC nanoparticles in region B are more than that in region A. In region B, uniformly dispersed crystal grains mount on the surface and the coating is basically even and compact. The region C is the aggregation area and lager grains stacked together. The SiC nanoparticles are typical second-phase material in composite coatings. The presence of SiC nanoparticles embedded into the metal or alloy matrix increased the wear resistance of the composite coatings. It shows that some agglomerations of SiC nanoparticles occurred in the plating bath and results in aggregation in the coating. Wu [29] reported that the higher microhardness nanoparticles improved the microhardness of the substrate to a greater extent than Ni coatings. They found that better corrosion resistance was obtained since the presence of TiN particles diminished the interspaces and improved the density of the coatings. It can be inferred that SiC nanoparticles might have the similar performances. EDS analysis shows that the

crystal aggregation contains more SiC nanoparticles. In composite electrodeposition, SiC nanoparticles can accelerate the growth of Ni-Co alloys to form stacked-like Ni-Co/SiC composites. Ni-Co/SiC nanocomposite coatings showed excellent mechanical properties such as hardness and anti-wear performance because of the high hardness of both Ni-Co matrix and SiC nanoparticles.

Therefore, it is expected that Ni-Co/SiC have a better protection performance and service life in marine environment. Although the highest content of SiC nanoparticles is in the crystal grain aggregation area, the aggregation is not SiC nanoparticles, but Ni-Co/SiC nanocomposites. As the nucleus and doping particles, SiC inclusion can initiate and promote the formation and growth of the Ni-Co/SiC grains and significantly change the structure of the composite coating. The distribution of SiC nanoparticles in the coatings is not uniform, which will impact the corrosion resistance, adhesion and wear resistance of the coating.

Nodular surface is partly attributed to the agglomerations of the nanoparticles and long deposition time. Also, another reason is that the aggregates adhered on the surface of the coatings have not been fully washed off after the deposits taken out of the electrolytes. In fact, the aggregations are not SiC nanoparticles, but Ni-Co/SiC composites. The imbedded SiC nanoparticles into Ni-Co matrix play an important role in determining the chemical composition and microstructure, and strengthen the microhardness of the composite coatings. SiC nanoparticles could initiate and accelerate the deposition process and obtain more even and compact coatings with better wear resistance and corrosion resistance, which is consistent with literatures [30].

3.2 Microstructure and composition of the nanocomposite coatings

Fig. 3 is the EDS spectrum of the composite coating. Fig. 3 (a) and (b) are the EDS of coatings prepared in the Ni-Co electrolyte solution with CoSO_4 concentration of 20 and 40 g/L respectively. It can be seen from Fig.3 (a) and (b), the coating contains Ni, Co elements and is Ni-Co alloy. A small amount of C may be formed by the deposition of carbon-containing complexes in the coating during electrodeposition. The Cu is due to the copper substrate. The Co content in the coating increased with the increase of Co^{2+} ions concentration in the electrolyte. When the concentration of CoSO_4 is 40 g / L, the atomic percentage of Co is 33.33%, which is 1.08% higher than that of 32.25% at 20 g/L. At the same time, the atomic percentage of Co/Ni increased from 47.03% to 70.27%. It was found that the Co content in the coating increased obviously as the increase of CoSO_4 concentration in the bath. Inclusion of Co in Ni matrix could modify the structure and physical properties of nickel alloy which could enhance the wear resistance, corrosion resistance and magnetic properties of the coatings.

Fig. 3(c) and (d) is the EDS of the Ni-Co/SiC nanocomposite coatings obtained by the addition of SiC ceramic nanoparticles in the Ni-Co electrolyte solution, according to the C, B region in Fig. 2. It can be seen that the coating contains Ni, Co, C, Si, O elements, indicates that the coating is Ni-Co/SiC nanocomposite coating. There is no Cu element in the map, indicating that the composite is compact and there is no obvious porosity and plating leakage. SEM analysis shows that there is a uniform SiC distribution area and aggregation area. In the crystal grain aggregation region, the growth of Ni-Co alloy can be accelerated by the heterogeneous nucleation of SiC nanoparticles, and Ni-Co/SiC stacked

composite will be produced. During the friction and wear process, the aggregation crystal is firstly rubbed. The wear resistance is improved because of the higher hardness of the SiC nanoparticles and the strengthening effects of the Co element on the nanocomposites, which extends the service life of the coating [31, 32]. After abrasion of the region C, the uniform area B, which is closer to the substrate, will bear the main load as the direct contacted surface. Then, more durable wear resistance and long service life were facilitated.

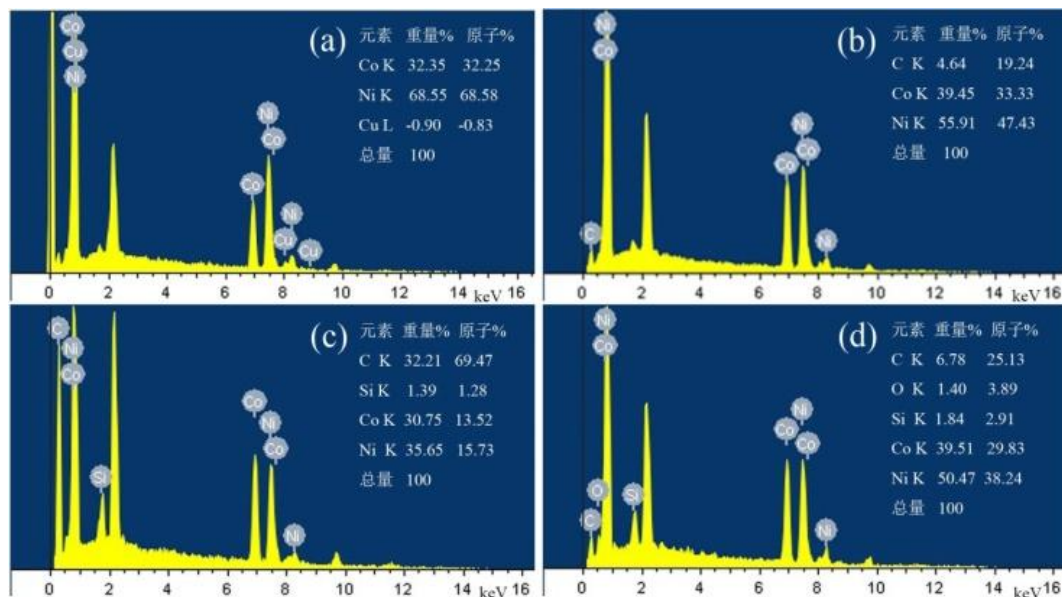


Figure 3. EDS spectrum of the Ni-Co alloys prepared with CoSO_4 (a) 20 g/L, (b) 40 g/L, (c) and (d) is Ni-Co/SiC alloys corresponding to C and B region in Fig.2 respectively.

Fig. 4 is the XRD patterns of the Ni-Co alloy coatings prepared in the bath containing different CoSO_4 concentration. Fig. 5 is the comparison of Ni-Co/SiC and Ni-Co XRD patterns. Ni-Co and Ni-Co/SiC composite coatings are mainly the structure of nickel face-centered cubic (fcc). Ni-Co deposits form solid solution through Co displaces a part of nickel atoms into the nickel crystal lattice. With the increase of Co^{2+} content, Ni content in the deposits decrease which facilitate the formation of amorphous structure. It can be seen from Fig.4 that the characteristic Ni peaks 2 and 3 become wider and lower as the increase of Co^{2+} concentration in the bath, and finally become the amorphous peak with the blunt shape, even disappear. The value of characteristic peak 1 of Ni also decreases with the increase of Co^{2+} , which indicates that the inclusion of Co^{2+} ions makes the composite structure amorphous. The amorphous structure is favorable for the improvement of corrosion resistance [33]. Fig.4 (f) is the XRD pattern of the Ni-Co-P alloy formed by the addition of P element, and it can be seen that the peak 1 broadens and the peaks 2, 3 and 4 is almost disappear. Thus, P has a positive effect on the amorphization of the coating.

Fig.5 is the XRD patterns of the Ni-Co/SiC nanocomposite coatings. It can be seen in Fig. 5 that Ni-Co/SiC composite coating is mainly composed by the Ni-Co alloy solid solution and SiC nanoparticles. It shows that with the addition of SiC nanoparticles, the blunt peak 4 becomes a sharp peak 3, the peak width is narrowed and the peak intensity increases, which shows that SiC

nanoparticles promote the crystal growth. With the process of electrodeposition, as heterogeneous nuclei, SiC nanoparticles can increase the number of nucleation, and promote the growth of crystallization. Peaks 1 and 2 in Fig. 5 are the characteristic peaks of the SiC nanoparticles in the crystals. The crystallization and the SiC nanoparticles improved the hardness of the coatings, which made them have better wear resistance. With the increasing of SiC nanoparticles in the solution, the formation of amorphous structure was facilitated. This result is similar with the findings of Pouladi [34].

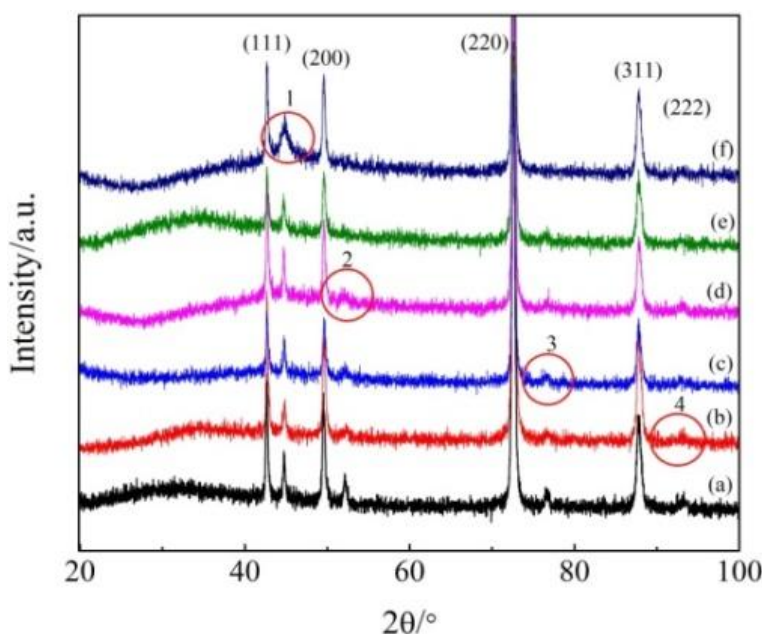


Figure 4. XRD diffraction pattern of the Ni-Co alloy coatings prepared in the bath containing CoSO_4 (a) 0, (b) 20, (c) 40, (d) 60, (e) 80 and (f) 60 g/L, and the (f) containing P element.

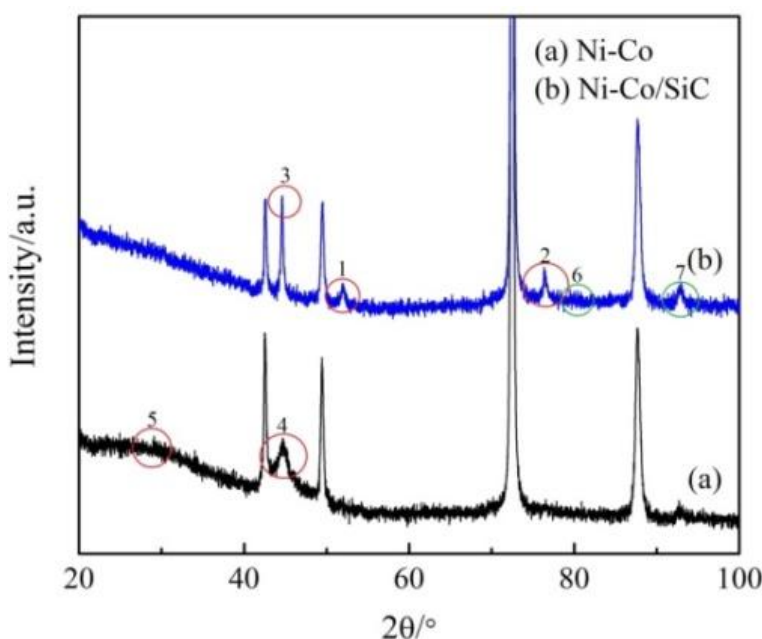


Figure 5. X-ray diffraction patterns of (a) Ni-Co alloys and (b) Ni-Co/SiC nanocomposite coatings.

The amorphous structure of the Ni-Co matrix implies two possible reasons regarding its structural characteristics. One is the formation of the amorphous Ni-Co structure by randomly incorporating Co atoms into the FCC lattice of Ni. The other is the growth of small nanocrystallites. The two structural changes could bring about positive effects on strengthening the composite coatings. Ni-Co/SiC composite coating shows the typical FCC lattice [35-37]. Ni-Co/SiC composite coating consists of Ni-Co alloy solid solution and SiC nanoparticles. There are amorphous, nanocrystal and nanoceramic SiC phase structure in the Ni-Co/SiC composite coating. As hardening element, SiC can strengthen the Ni-Co matrix which has better wear resistance.

3.3 Corrosion resistance of the nanocomposite coatings

With strong adhesion force between the coating and the matrix, the coatings and embedded SiC nanoparticles are not easy to be peeled off. Therefore, the adhesion force is one of the key factors for the coating performance and has great effect on the corrosion properties [38, 39]. It can be seen in table 2 that the drop rate of Ni-Co/SiC nanocomposite coating is generally less than 5%, which is obviously lower than that of Ni-Co alloy coating. SiC nanoparticles not only have no deleterious effect on the adhesion of Ni-Co alloy, but also can improve the adhesion of the coating. This is probably due to the high hardness of SiC nanoparticles, which plays the role of bonding backbone. Since SiC nanoparticles is much smaller than the micron level Ni-Co composite crystals, the SiC nanoparticles can fill the interspace between Ni and Co so that the coating is more compact.

Table 2. Adhesion test results of coats

coatings	Peel off percent	ASTM grade
Ni-Co	5%~15%	3B
Ni-Co/SiC	≤5%	4B

EIS results further demonstrated that the corrosion resistance of the nanocomposite coatings is generally higher than Ni and Ni-Co coatings. The Nyquist plots of Ni-Co and Ni-Co-SiC nanocomposite coating immersed in neutral 3.5 wt.% NaCl solution for different times are presented in Fig.6. It shows that the Nyquist plots have the similar shapes of depressed semicircle arc with different radius. It is generally believed that the larger the radius of the semicircle arc in the curves, the greater the polarization resistance (R_p), and the better the corrosion resistance. As shown in Fig.6, the polarization resistance (R_p) value decreases with the increase of immersion time, and the corrosion resistance of the coating decreases too. The results also indicated that SiC nanoparticles modified the microstructure of the electrodeposited coatings. This enhances the corrosion resistance of the deposits as physical barriers to inhibit the germination and expanding of the corrosion [23]. The higher corrosion resistance of Ni-Co/SiC than that of Ni-Co coatings can be certified by EIS results when immersed in the neutral 3.5 wt.% NaCl solutions for 1 to 30 days at open circuit potential. These Nyquist plots in Fig. 6 are similar, which contain one high frequency capacitive arc. It can be observed that the radius of the semicircle arc for Ni-Co/SiC is obvious bigger than that of Ni-Co coatings. This

indicates that the corrosion resistance of Ni-Co/SiC is better than Ni-Co coating. As seen in Fig.6(a), the impedance R_c of the Ni-Co alloys increases with the immersion time in the first three days, and then decreases with the extending of immersion time. After immersed 15 days, the R_c value decreases fast. When 20 days, the impedance R_c decrease slowly and is gradually constant. In the initial 10 days, the resistance value of Ni-Co is better or the same to Ni-Co/SiC. After immersed 10 days, the corrosion resistance of Ni-Co deposits is already lower than Ni-Co/SiC nanocomposites. After 20 days, the impedance value of Ni-Co/SiC nanocomposite was obviously better than Ni-Co coatings. Pouladi et al [27] pointed out that the EIS charge transfer resistance values of Ni-W/SiC composite coatings were higher compared to pure Ni-W coating, and the increase in SiC concentration led to a decrease in corrosion current density and thereby increase in corrosion potential. The corrosion resistance of as-prepared Ni-Co is better in the early service stage. However, the corrosion resistance of Ni-Co decreases rapidly with the immersed time, which may be due to the cracks or pinholes structure of the coating. The impermeability of the Ni-Co coating is insufficient to maintain high corrosion resistance for a long period of time. Therefore, the Ni-Co/SiC nanocomposite has better service stability and durability than Ni-Co coatings.

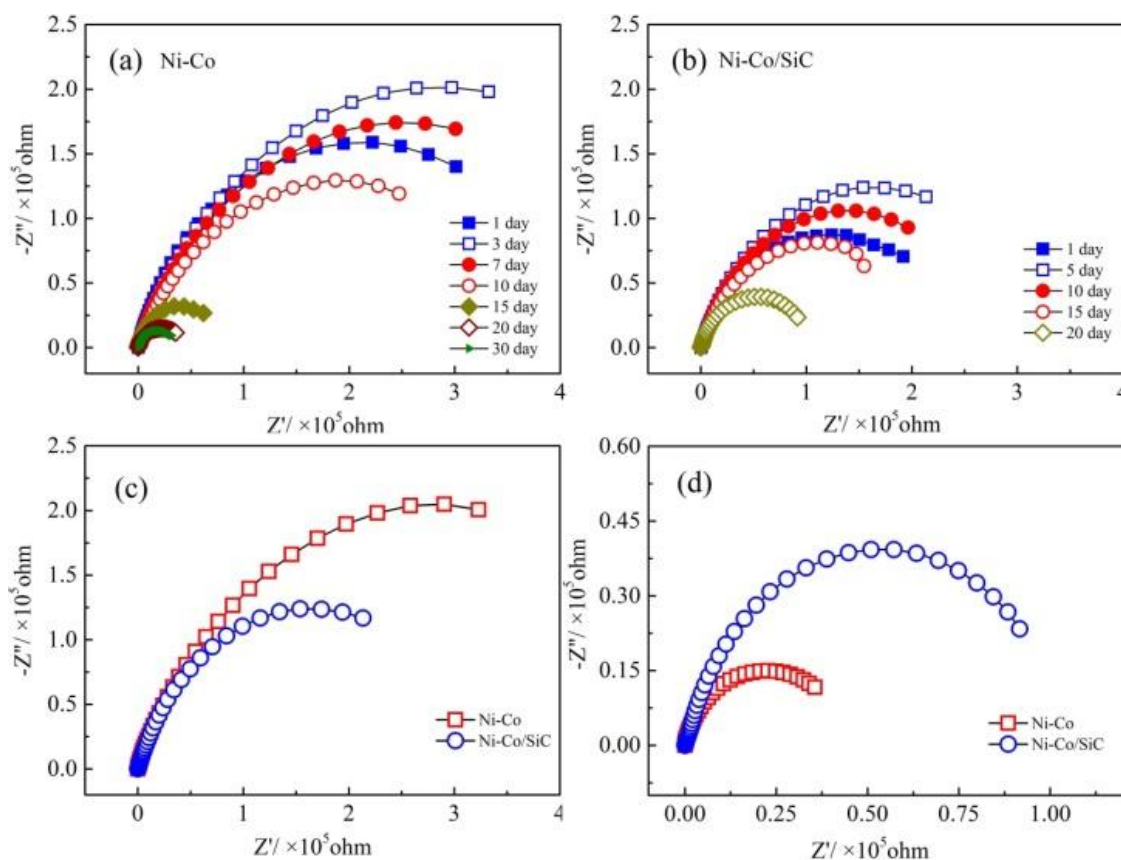


Figure 6. (a) and (b) is Nyquist plots corresponding to Ni-Co, Ni-Co/SiC coatings after immersion in 3.5% NaCl solution for different days, (c) and (d) is the plots immersed 5 and 20 days respectively.

Fig.7 is the polarization curve of the nanocomposites immersed in 3.5% NaCl solution for different time, and the corresponding $E_{ocp}-t$ curve is embedded in the right-down side of the figure. It can be seen from Fig. 7 that the corrosion potential of the coating is unstable during the immersion process due to the heterogeneous structure of the coating. At the beginning of immersion, the corrosion potential of Ni-Co alloys decreased rapidly from -0.1701 V to the lowest -0.2414 V when immersed 10 days. E_{corr} increased to -0.1983 V at 15 days. Thereafter, E_{corr} of Ni-Co alloy decreased slowly and was -0.2296V at 30 days. The initial corrosion potential of the Ni-Co/SiC alloy as seen from polarization curve is -0.2074 V, which increases to -0.1771 V at 3 days, decreases to -0.2439V at 10 days, reaches -0.1924 V at 15 days and then decrease slowly. When immersed 30 days, the corrosion potential was -0.2377 V. The increase of E_{ocp} at 10 days may be due to the change of the interface between the coating and the electrode. With the transport of the electrolyte in the coating, the corrosion control stage was changed from the diffusion step to the electrochemical control step. Therefore, the corrosion of the coating experienced three stages, namely the wetting stage, diffusion control stage which electrolyte transport in the coating and electrochemical control stage in which diffusion process is larger than that of electrochemical's [8]. The first stage is the electrode wetting stage, including the bath solution wetting the microstructure of the coating surface, such as the $E_{ocp}-t$ curve of the first 3 days for Ni-Co/SiC. Then enter the second stage, the electrolyte gradually penetrate and transport in the coating, which is the diffusion step control stage; When the electrolyte reaches the substrate surface, the substrate surface accumulated a large number of electrolyte ions. In this stage, the diffusion rate has been greater than the electrochemical reaction rate, in which the electrochemical process is the corrosion control steps.

The corrosion potential E_{corr} , the corrosion current density i_{corr} and the linear polarization resistance R_{lp} can be obtained by fitting the above polarization curves. As seen from Table 3, when immersed 30 days, the corrosion potential E_{corr} of Ni-Co/SiC composite coating is -0.266 V and the corrosion current i_{corr} is $2.63 \times 10^{-7} \text{ A}\cdot\text{cm}^{-2}$, the linear polarization resistance R_{lp} is $120.6 \text{ k}\Omega\cdot\text{cm}^2$. It indicates that with the inclusion of SiC nanoparticles, the corrosion potential of Ni-Co/SiC coating is more positive, the corrosion current is decreased, the linear polarization resistance is higher, and the corrosion resistance is better.

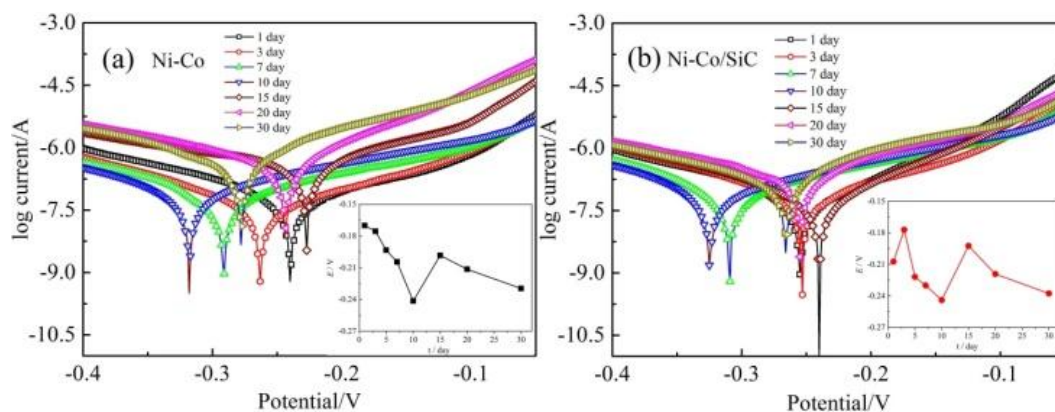


Figure 7. TAFEL polarization and $E_{ocp}-t$ curves (a) Ni-Co (b) Ni-Co/SiC

Table 3. Corrosion data extracted from potentiodynamic polarization plots in Fig.7

	Immersed days	E_{corr} (mV)	i_{corr} ($\mu\text{A cm}^{-2}$)	R_p ($\text{k}\Omega \text{cm}^2$)
NiCo	1	-240	0.071	413.3
	3	-263	0.045	581.1
	7	-291	0.081	407.2
	10	-318	0.104	318.0
	15	-227	0.603	618.0
	20	-244	0.450	54.1
	30	-278	0.566	52.0
Ni-Co/SiC	1	-255	0.049	412.0
	3	-253	0.081	322.2
	7	-309	0.099	303.5
	10	-325	0.104	294.2
	15	-240	0.056	373.2
	20	-255	0.316	103.3
	30	-266	0.263	120.6

The presence of SiC nanoparticles enhances the wear resistance and restrains the matrix dissolution, then significantly improves the corrosion resistance. Except for the positive shift of the corrosion potential, the corrosion rate also decreases with the inclusion of SiC into the coating. Co-deposited into the coatings, SiC can fill the interval space between the grains of the alloy matrix, and act as a compact barrier and resist the corrosion attack [40, 41]. In addition, it is needed to point out that grain refinement strengthens the corrosion resistance. In nanocomposite coatings, grain boundaries could also act as suitable sites for nucleation and growth of passive films. Then, more stable and protective passive films would be formed which will indirectly improve the corrosion resistance of the coating [42].

4. CONCLUSIONS

In the present study, Ni-Co/SiC nanocomposite coatings were prepared by electrodeposition from a Ni-Co electrolyte containing suspended SiC nanoparticles. The microstructure, electrodeposition parameters and corrosion properties of Ni-Co and Ni-Co/SiC nanocomposite coatings were investigated. The co-deposition of Co into the Ni matrix could refine the crystal grains, decrease the porosity, and finally improved the corrosion resistance. Ni-Co/SiC composite coatings showed excellent mechanical properties because of the high hardness of both Ni-Co matrix and SiC nanoparticles. Ni-Co/SiC nanocomposite coatings were prepared by inclusion of SiC nanoparticles into Ni-Co alloy matrix, which lead to better corrosion and wear resistance than Ni-Co alloys. EIS results show that Ni-Co/SiC exhibits more excellent long-term service stability than Ni-Co alloys. The electrodeposited nanocomposite coating has good wear resistance and anti-corrosion behavior, which can provide long-term protection for marine machinery under the multifactor interaction in marine environment. It has a good application prospect in marine protection field.

ACKNOWLEDGEMENTS

The authors gratefully acknowledge financial support from the National Natural Science Foundation of China (No. 51679076, 51605137, 51301061).

References

1. W. Sassi, L. Dhouibi, P. Berçot, M. Rezrazi, E. Triki, *Surf. Coat. Technol.*, 206 (2012) 4235.
2. S. Singh, M. Sribalaji, N.P. Wasekar, S. Joshi, G. Sundararajan, R. Singh, A.K. Keshri, *Microstructural, Appl. Surf. Sci.*, 364 (2016) 264.
3. B. Bakhit, A. Akbari, F. Nasirpouri, M.G. Hosseini, *Appl. Surf. Sci.*, 307 (2014) 351.
4. C.M.P. Kumar, T.V. Venkatesha, R. Shabadi, *Mater. Res. Bull.*, 48 (2013) 1477.
5. M.H. Fini, A. Amadeh, *Trans. Nonferrous Met. Soc. China*, 23 (2013) 2914.
6. D. Eroglu, A. Vilinska, P. Somasundaran, A.C. West, *Electrochim. Acta*, 113 (2013) 628.
7. B. Bahadormanesh, A. Dolati, M.R. Ahmadi, *J. Alloys Compd.*, 509 (2011) 9406.
8. L.L. Tian, J.C. Xu, C.W. Qiang, *Appl. Surf. Sci.*, 257 (2011) 4689.
9. Y.H. You, C.D. Gu, X.L. Wang, J.P. Tu, *Surf. Coat. Technol.*, 206 (2012) 3632.
10. Y.W. Yao, S.W. Yao, L. Zhang, H.Z. Wang, *Mater. Lett.*, 61 (2007) 67.
11. N. Spyrellis, E.A. Pavlatou, S. Spanou, A. Zoikis-Karathanasis, *Trans. Nonferrous Met. Soc. China*, 19 (2009) 800.
12. M.D. Ger, *Mater. Chem. Phys.*, 87 (2004) 67.
13. Y. Zhou, H. Zhang, B. Qian, *Appl. Surf. Sci.*, 253 (2007) 8335.
14. B. Bakhit, A. Akbari, *Surf. Coat. Technol.*, 253 (2014) 76.
15. H. Ogihara, H. Wang, T. Saji, *Appl. Surf. Sci.*, 296 (2014) 108.
16. Y. Yang, Y.F. Cheng, *Electrochim. Acta*, 109 (2013) 638.
17. Y.J. Xu, Y.Y. Zhu, G.R. Xiao, C.Y. Ma, *Ceram. Int.*, 40 (2014) 5425.
18. J.L. Wang, R.D. Xu, Y.Z. Zhang, *Trans. Nonferrous Met. Soc. China*, 20 (2010) 839.
19. A. Zoikis-Karathanasis, E.A. Pavlatou, N. Spyrellis, *J. Alloys Compd.*, 494 (2010) 396.
20. S. Sadreddini, A. Afshar, *Appl. Surf. Sci.*, 303 (2014) 125.
21. S.Y. Chiu, S.T. Chung, C.Y. Lin, W.T. Tsai, *Surf. Coat. Technol.*, 247 (2014) 68.
22. F.F. Xia, Z.Y. Jia, M.H. Wu, F. Wang, F. Huo, *Rare Met. Mater. Eng.*, 37 (2008) 1479.
23. B. Bakhit, *Surf. Coat. Technol.*, 275 (2015) 324.
24. I. Garcia, J. Fransaeer, J.P. Celis, *Surf. Coat. Technol.*, 148 (2001) 171.
25. Z.C. Guo, X.Y. Zhu, D.C. Zhai, X.W. Yang, *J. Mater. Sci. Technol. (Shenyang, China)*, 16 (2000) 323.
26. K.A. Kumar, G.P. Kalaigan, V.S. Muralidharan, *Trans. Inst. Met. Finish.*, 91 (2013) 202.
27. M.G. Hosseini, M. Abdolmaleki, J. Ghahremani, *Corros. Eng., Sci. Technol.*, 49 (2013) 247-253.
28. L.M. Chang, H.F. Guo, M.Z. An, *Mater. Lett.*, 62 (2008) 3313-3315.
29. F.F. Xia, C. Liu, F. Wang, M.H. Wu, J.D. Wang, H.L. Fu, J.X. Wang, *J. Alloys Compd.*, 490 (2010) 431.
30. X.K. He, B.L. Hou, L.Y. Wu, B.Z. Chen, *Rare Met. Mater. Eng.*, 43 (2014) 1742.
31. S. Khorsand, K. Raeissi, F. Ashrafizadeh, M.A. Arenas, *Surf. Coat. Technol.*, 276 (2015) 296.
32. A. Laszczyńska, J. Winiarski, B. Szczygieł, I. Szczygieł, *Appl. Surf. Sci.*, 369 (2016) 224.
33. C. Ma, S.C. Wang, L.P. Wang, F.C. Walsh, R.J.K. Wood, *Surf. Coat. Technol.*, 235 (2013) 495.
34. S. Pouladi, M.H. Shariat, M.E. Bahrololoom, *Surf. Coat. Technol.*, 213 (2012) 33.
35. E. Beltowska-Lehman, P. Indyka, A. Bigos, M. Kot, L. Tarkowski, *Surf. Coat. Technol.*, 211 (2012) 62.
36. K.H. Hou, T.W. Han, H.H. Sheu, M.D. Ger, *Appl. Surf. Sci.*, 308 (2014) 372.
37. L. Elias, A. Chitharanjan Hegde, *Surf. Coat. Technol.*, 283 (2015) 61.
38. Y. Yang, Y.F. Cheng, *Surf. Coat. Technol.*, 205 (2011) 3198.

39. B. Bakhit, A. Akbari, *Surf. Coat. Technol.*, 206 (2012) 4964.
40. M. Srivastava, V.K.W. Grips, K.S. Rajam, *Appl. Surf. Sci.*, 253 (2007) 3814.
41. B. Bakhit, A. Akbari, *J. Alloys Compd.*, 560 (2013) 92.
42. Z. Wu, B. Shen, L. Liu, *Surf. Coat. Technol.*, 206 (2012) 3173.

© 2017 The Authors. Published by ESG (www.electrochemsci.org). This article is an open access article distributed under the terms and conditions of the Creative Commons Attribution license (<http://creativecommons.org/licenses/by/4.0/>).